HHS Public Access

Author manuscript

Gastroenterology. Author manuscript; available in PMC 2024 June 01.

Published in final edited form as:

Gastroenterology. 2023 June ; 164(7): 1279–1292. doi:10.1053/j.gastro.2023.02.043.

A therapeutically targetable TAZ-TEAD2 pathway drives the growth of hepatocellular carcinoma via ANLN and KIF23

Yoshinobu Saito[†,*],
Associate Research Scientist, Department of Medicine, Columbia University, New York, NY 10032, USA

Dingzi Yin[†],
Postdoctoral Fellow, Division of Gastroenterology, Department of Medicine, University of Pennsylvania Perelman School of Medicine, Philadelphia, PA 19104, USA. Current address: Division of Gastroenterology and Hepatology, Department of Medicine, Mayo Clinic, Rochester, MN 55905, USA

Naoto Kubota,
Postdoctoral Fellow, Division of Digestive and Liver Diseases, Department of Internal Medicine, University of Texas Southwestern Medical Center, Dallas, TX 75390, USA.

Xiaobo Wang,
Assistant Professor, Department of Medicine, Columbia University, New York, NY 10032, USA.

Aveline Filliol,
Associate Research Scientist, Department of Medicine, Columbia University, New York, NY 10032, USA

Helen Remotti,
Associate Professor, Department of Pathology and Cell Biology, Columbia University Irving Medical Center, New York, NY 10032, USA

Ajay Nair,

[*]**Correspondence to**: Robert F. Schwabe, 1130 St. Nicholas Ave, ICRC, Room 926, New York, NY 10032; phone: 001-212-851-5462; rfs2102@cumc.columbia.edu, Kirk J. Wangensteen, Division of Gastroenterology and Hepatology, Mayo Clinic, 200 First ST SW, Rochester, MN 55905; phone: 001-507-293-2698; wangensteen.kirk@mayo.edu, Yoshinobu Saito, 1130 St. Nicholas Ave, ICRC, Room 916B, New York, NY 10032; phone: 001-212-851-5464; ys3261@cumc.columbia.edu.
[†]Authors contributed equally to the study.

AUTHOR CONTRIBUTIONS. Y.S. conceived, designed experiments, generated, analyzed, and interpreted data, and drafted the manuscript. D.Y designed experiments, generated the flox-removed dCas9 mice, generated, analyzed and interpreted data related to CRISPRi screening. X.W. contributed to experiments involving ChIP, cholesterol loading and depletion and NASH-induced HCC. A.F. designed experiments, generated data related to DEN+CCl_4-induced HCC. H.R. and L.F. generated tissue microarrays and histopathologically evaluated liver tumors. A.N. contributed to analysis of TCGA-LIHC data. N.K. and Y.H contributed to analysis of TCGA-LIHC and ICGC-LIRI-JP data. K.W. generated dCas9 mice, supervised CRISPRi screening and edited the manuscript. I.T. supervised on studies involving ChIP, cholesterol loading and depletion and NASH-induced HCC and edited the manuscript. R.F.S. conceived and oversaw the study, designed experiments, drafted and edited the manuscript.

Author names in bold designate shared co-first authorship" at the end of the references section.

Data Transparency Statement: All data will be made available immediately after publication.

Writing Assistance: None.

Associate Research Scientist, Department of Medicine, Columbia University, New York, NY 10032, USA

Ladan Fazlollahi,
Assistant Professor of Pathology and Cell Biology, Columbia University Irving Medical Center, New York, NY 10032, USA

Yujin Hoshida,
Professor, Division of Digestive and Liver Diseases, Department of Internal Medicine, University of Texas Southwestern Medical Center, Dallas, TX 75390, USA.

Ira Tabas,
Professor, Department of Pathology and Cell Biology, Columbia University Irving Medical Center, New York, NY 10032, USA, Institute of Human Nutrition, New York, NY 10032, USA.

Kirk J. Wangensteen*,
Assistant Professor, Division of Gastroenterology, Department of Medicine, University of Pennsylvania Perelman School of Medicine, Philadelphia, PA 19104. Current address: Assistant Professor, Division of Gastroenterology and Hepatology, Department of Medicine, Mayo Clinic, Rochester, MN 55905.

Robert F. Schwabe*
Professor, Department of Medicine, Columbia University, New York, NY 10032, USA, Institute of Human Nutrition, New York, NY 10032, USA.

Abstract

Background and Aims: Despite recent progress, long-term survival remains low for hepatocellular carcinoma (HCC). The most effective HCC therapies target the tumor immune microenvironment (TIME), and there are almost no therapies that directly target tumor cells. Here, we investigated the regulation and function of tumor cell-expressed YAP and TAZ in HCC.

Methods: HCC was induced in mice by *Sleeping Beauty*-mediated expression of MET, CTNNB1-S45Y or TAZ-S89A, or by diethylnitrosamine plus CCl_4. Hepatocellular TAZ and YAP were deleted in floxed mice via AAV8-TBG-Cre. TAZ target genes were identified from RNA-seq, confirmed by ChIP and evaluated in a CRISPRi screen. TEADs, Anln, Kif23 and PD-L1 were knocked down by guide RNAs in dead Cas9 knock-in mice.

Results: YAP and TAZ were upregulated in murine and human HCC, but only deletion of TAZ consistently decreased HCC growth and mortality. Conversely, overexpression of activated TAZ was sufficient to trigger HCC. TAZ expression in HCC was regulated by cholesterol synthesis as demonstrated by pharmacologic or genetic inhibition of HMGCR, FPPS, FDFT1, or SREBP2. TAZ- and MET/CTNNB1-S45Y-driven HCC required the expression of TEAD2 and, to a lesser extent, TEAD4. Accordingly, TEAD2 displayed the most profound effect on survival in HCC patients. TAZ and TEAD2 promoted HCC via increased tumor cell proliferation, mediated by TAZ target genes ANLN and KIF23. Therapeutic targeting of HCC, using pan-TEAD inhibitors or the combination of a statin with either sorafenib or anti-PD-1, decreased tumor growth.

Conclusions: Our results suggest the cholesterol-TAZ-TEAD2-ANLN/KIF23 pathway as mediator of HCC proliferation and tumor cell-intrinsic therapeutic target that could be synergistically combined with TIME-targeted therapies.

Lay summary

We identified a tumor-promoting TAZ-TEAD2-ANLN/KIF23 pathway in HCC. Targeting this pathway in tumor cells, e.g. by TEAD inhibitors or statins, showed therapeutic effects and can potentially be combined with already approved HCC therapies that target non-tumor cells.

Keywords

Liver cancer; statin; CRISPR; immune checkpoint inhibition; combination therapy; tyrosine kinase inhibitor; VT104; VT107; anillin; kinesin family member 23

Introduction

Hepatocellular carcinoma (HCC) represents the fourth most common cause of cancer-related mortality, causing approximately 800,000 deaths/year world-wide [1]. Its incidence has tripled in the US and Western counties in the last three decades[2] and a further rise is expected due to increasing rates of non-alcoholic fatty liver disease (NAFLD). The increasing HCC death rates in the US contrast the decreasing mortality for most solid cancers[3]. Despite recent advances in the medical therapy of advanced HCC[4–7], median survival is still below two years even with the most effective medical therapies, making this an important unmet need in medicine. The most effective therapies for advanced HCC, such as immune checkpoint inhibitors (ICI) and their combination with vascular endothelial growth factor (VEGF) inhibition[6], target the tumor immune microenvironment (TIME) instead of direct targeting tumor cells. Moreover, only about 20–25% of HCCs contain actionable mutations[8].

Here, we investigated YAP and TAZ as well as their upstream and downstream mediators as tumor cell-intrinsic pathways that are commonly activated and could be therapeutically targeted. While YAP and TAZ are well-established tumor promoters in a wide range of organs including the liver[9,10], the specific contribution of YAP versus TAZ is not as well understood in liver cancer. We have previously shown a role for hepatocyte TAZ in the development in non-alcoholic steatohepatitis (NASH)[11,12] and the transition to NASH-HCC[13]. In established HCC, TAZ is highly expressed[14] and may predict HCC patient survival[15]. However, most functional studies have focused on YAP deletion[16,17] or compound deletion[18] of YAP and TAZ. The mechanisms of YAP and TAZ upregulation and their downstream targets in HCC are not well understood, and may reveal novel therapeutic targets. Our study shows that TAZ expression in HCC is regulated by the mevalonate-cholesterol pathway. TAZ but not YAP is the key determinant of HCC growth and sufficient to trigger HCC growth in mice. Tumor-promoting effects of TAZ were mediated by its interaction partner TEAD2 and TAZ target genes anillin (ANLN) and kinesin family member 23 (KIF23*).* Therapeutic targeting of this pathway by statins, pan-TEAD inhibitors or the combination of statins with anti-PD-L1 reduced tumor growth.

MATERIAL AND METHODS

Study approval.

Samples for human tissue microarray (TMA) construction were collected from patients with written informed consent. Patient records were anonymized and de-identified. The study was approved by Columbia University Medical Center Institutional Review Board (Protocol Number: IRB-AAAN2452) and conduced in accordance with National Institutes of Health and institutional guidelines for human subject research. All animal procedures were performed with approval by the Columbia University IACUC (protocols AC-AAAV2454, AC-AABM2555 and AC-AABQ5565) or University of Pennsylvania IACUC (protocol 806401) and were in accordance with the Guide for the Care and Use of Laboratory Animals.

Induction of hepatocarcinogenesis

For genotoxic HCC, 15-day-old male mice were intraperitoneally injected with 25 mg/kg diethylnitrosamine (Sigma, N0756) followed by 15 weekly CCl_4 injections (0.5 mL/kg, i.p. in corn oil) starting at 6–8 weeks of age. For YAP- or TAZ-driven HCC, male mice were injected by hydrodynamic tail vein injection (HTVI) with 20 μg pT3-EF1a-TAZS89A or 20 μg pT3-EF1a-YAPS127A together with 5 μg of pCMV-SB13 plasmid, or with 25 μg pKT2-EF1a-TAZS89A/U6-gRNA/PGK-SB11, which was generated by cloning EF1a-TAZS89A/U6-gRNA/PGK-SB11 into pKT2 *Sleeping Beauty* plasmid[19]. For the induction of oncogene-driven HCC, a combination of 20 μg pT3-EF1a-MET, 20 μg pT3-EF5a-CTNNB1-S45Y-Myc-tag and 10 μg of pCMV-SB13 plasmid was injected into male mice at six to seven weeks of age by HTVI. To evaluate tumor burden of mice, the liver weight to body weight (LW/BW) ratio, tumor numbers and average of the three biggest tumors were determined, as well as the CTNNB1-Myc-Tag-positive area for some experiments.

CRISPR interference (CRISPRi) screening

CRISPRi screening was performed in dead Cas9 (dCas9) transgenic mice using a TAZ-CRISPRi plasmid library, described in the further details in the supplementary methods.

Statistics

Data are shown as mean±SEM unless otherwise indicated. GraphPad Prism v.9.0 or R version 4.2.1 were used for statistical analysis. Distribution normality was tested by Anderson-Darling, D'Agostino&Pearson omnibus, Shapiro-Wirk and Kolmogorov-Smirnov tests. For parametric data, two-tailed unpaired Student t-test and one-way ANOVA followed by Turkey's or Dunnette's multiple comparison test were performed for two groups and three or more groups, respectively. For non-parametric data, Mann-Whitney test and Kruskal-Wallis test followed by Dunn's multiple comparison test were performed for two groups and three or more groups, respectively, unless otherwise indicated.

Data availability

Data sets related to identifying YAP/TAZ/TEAD target genes in TAZ+CCl_4-induced tumors vs normal liver with RNA-seq are available at Gene Expression Omnibus (GEO), identifier GSE224173 (https://www.ncbi.nlm.nih.gov/geo/query/acc.cgi?&acc=GSE224173).

RESULTS

TAZ, not YAP, deletion strongly reduces HCC development and mortality.

TAZ and YAP were significantly upregulated in multiple mouse models of HCC (Fig.1A–B, Suppl.Fig.1A) and in the majority of human HCCs (50%, i.e. 31 of 62 cases) as demonstrated by immunohistochemistry in a human tissue microarray (TMA) (Fig.1C, Suppl.Fig.1B–C). Of note, TMA cases showed no difference in TAZ expression as well as the Sirius Red-, CD3- and CD45-positive areas between viral and non-viral etiologies (Suppl.Fig.1D–G). Surprisingly, hepatocyte-specific deletion of YAP via adeno-associated virus serotype 8 (AAV8)-mediated thyroxin-binding globulin (TBG)-driven Cre expression (AAV8-TBG-Cre), despite being highly efficient (Suppl. Fig.2A), had a negligible effect on tumor growth and survival in oncogene-driven HCC, induced by HTVI of *Sleeping Beauty* plasmids (Fig.1D). In contrast, hepatocyte-specific TAZ deletion (Suppl.Fig.2A) significantly reduced tumor growth and improved survival in the MET+CTNNB1-S45Y HCC model (Fig.1E). Similar roles for YAP and TAZ were confirmed in the DEN+CCl_4 genotoxic HCC model (Suppl.Fig.2B). Overexpression of degradation-resistant activated TAZ (TAZ-S89A) was sufficient to trigger HCC development 4 months after HTVI, whereas degradation-resistant YAP-S127A [20–22] induced small tumors only in a minority of mice (Fig. 1F). TAZ-S89A-induced tumors were grade 3–4 HCC, with typical reticulin and AFP staining and increased *Gpc3* and *Afp* mRNA (Fig. 1G). In conclusion, our complementary approaches suggest TAZ as a more potent regulator of HCC growth compared to YAP.

The mevalonate-squalene-cholesterol biosynthesis pathway regulates TAZ expression in HCC.

We next sought to understand how TAZ activity is regulated in driving HCC. MET+CTNNB1-S45Y-induced HCCs occur in the absence of strong fibrosis (Suppl.Fig.2D) and are relatively soft, suggesting that factors other than stiffness, a well-known regulator of TAZ and YAP[23], may contribute to the upregulation of TAZ. It was recently reported that cholesterol regulates TAZ expression in hepatocytes and contributes to the development of experimental non-alcoholic steatohepatitis (NASH)[12]. Different from primary hepatocytes[12] and AML12 cells (Suppl.Fig.3A), the addition of exogenous cholesterol to cholesterol-depleted cells did not increase TAZ expression in HCC lines, Huh7 and PLC/PRF/5 (Fig.2A). However, inhibition of cholesterol synthesis via pharmacological inhibition or silencing of 3-hydroxy-3-methylglutaryl-CoA reductase (HMGCR) strongly reduced TAZ expression in HCC lines (Fig.2B, Suppl.Fig.3B). In addition to cholesterol biosynthesis, the mevalonate pathway also provides substrates for geranyl-geranylation and farnesylation, which have been shown to regulate YAP and TAZ expression[24]. Systemic investigation of this pathway, using both pharmacologic inhibition and genetic silencing revealed that inhibition of farnesyl pyrophosphate synthase (FPPS) by Zoledronic acid, and inhibition of farnesyl-diphosphate farnesyltransferase 1 (FDFT1) by YM-53601 or silencing

of SREBP2, a master regulator of cholesterol synthesis[25,26] and contributor to HCC development[27,28], reduced TAZ expression (Fig.2C, Suppl.Fig.3C). In contrast, inhibition of farnesyl transferase via FTI-277 and of geranyl-gernanyltransferase via GGTI-298 did not (Fig.2B, Suppl.Fig.3B). Conversely, provision of the cholesterol metabolites, mevalonate, FPP and squalene, but not GGPP, increased TAZ expression in Huh7 cells but not in primary hepatocytes (Suppl.Fig.3D–E). To test the hypothesis that endogenous cholesterol synthesis regulates TAZ expression and HCC growth *in vivo*, we subjected mice with hepatocyte-specific SREBP2 deletion, achieved via injection of AAV8-TBG-Cre or AAV8-TBG-Null in *Srebp2*$^{fl/fl}$ mice one week before HTVI of MET+CTNNB1-S45Y plasmids (Fig.2D). SREBP-2 deletion significantly reduced TAZ expression four weeks after hydrodynamic tail vein injection, i.e. at a time where macroscopic tumors had not yet developed (Fig.2D) and suppressed HCC growth at later time points (Fig.2E).

The cholesterol-TAZ-TEAD2 pathway promotes HCC development by driving proliferation.

TAZ and YAP are transcriptional co-activators that interact with several transcriptional factors to regulate gene expression[21]. In addition to TEADs[29], YAP and TAZ may also mediate downstream effects through SMAD1[30], SMAD2/3[31,32] and T-box transcription factor 5 (TBX5)[33]. To clarify the role of TEAD-dependent versus TEAD-independent signals in hepatocarcinogenesis, we first overexpressed TAZ-S51A, which lacks interactions with TEADs[34]. HTVI of pT3-EF1a-TAZ-S89A-S51A alone or followed by 30 CCl_4 injections did not induce HCC while HTVI of pT3-EF1a-TAZ-S89A alone 4 months later or followed by CCl_4 injection induced HCC (Fig.3A), suggesting a crucial role for TAZ-TEAD interaction in HCC development. To study the role of the different TEADs in HCC development, we targeted each of the TEADs separately in dCas9 knock-in mice, using CRISPR interference (CRISPRi)[35] via HTVI of a *Sleeping Beauty* plasmid co-expressing guide RNAs (gRNA) with activated TAZ (EF1a-TAZ-S89A-U6-gRNA). The gRNAs targeting Tead1–4 were validated in a dCas9 transgenic murine HCC line (Suppl.Fig.4A). Inhibiting *Tead2* and *Tead4* via CRISPRi significantly reduced TAZ-driven tumor growth, whereas *Tead1*, *Tead3* did not (Fig.3B). Next, we tested the role of each TEAD in MET+CTNNB1-S45Y HCC as a model that driven by common oncogenes. Again, Tead2 emerged as a key driver of HCC growth, suppressing all readouts for HCC growth, whereas Tead3 showed only a trend towards HCC reduction and Tead1 and Tead4 negligible effects on HCC growth in this model (Suppl.Fig.4B). Analysis of data from The Cancer Genome Atlas (TCGA), and confirmed in a second cohort from the International Cancer Genome Consortium (ICGC), revealed that high *TEAD2* and *TEAD4* expression levels were significantly associated with decreased survival in HCC patients, and that *TEAD2* and *TEAD3* were significantly associated with recurrence-free survival (Fig.3C, Suppl.Fig.5A–B). *TEAD1, TEAD2, TEAD3 and TEAD4* expression did not differ significantly between different etiologies of HCC in the TCGA dataset, and high TEAD2 expression was significantly associated with survival in non-viral HCC and showed strong trends towards lower survival viral HCC, while higher TEAD4 levels were associated with decreased survival in viral HCC, but show a strong trend towards increased survival in non-viral HCC (Suppl.Fig.6A–B). Given the central role of TEAD2 in both mouse models and patients, we investigated whether an active form of Tead2, achieved by fusion to transcriptional activator VP-16 (Tead2-VP16)[36] is sufficient to trigger HCC development. Similar to

TAZ, overexpression of Tead2-VP16, but not dominant negative (dnTead2) or GFP, triggered HCC development, but only when combined with CCl_4 or NASH diet (Fig.3D, Suppl.Fig.4C). These data suggest that TAZ-S89A is either more potent than TEAD2 or that upregulation of TEAD2 interaction partner TAZ by high-dose $CCl_4$37 or NASH diet[11] is required for TEAD2 pro-tumorigenic effects. Next, we investigate the mechanism by which TAZ and TEAD induce tumorigenesis. TAZ deletion, and TAZ reduction via *Srebp2* deletion significantly reduced Ki67-positive hepatocytes and hepatocytes positive for DNA damage marker γH2AX (Fig.3E, Suppl.Fig.7A–B). Conversely, overexpression of TAZS89A or TAZS89A-IRES-GFP, which also efficiently triggered HCC, or overexpression Tead2-VP16 in combination with CCl_4 significantly increased Ki67-positive and γH2AX-positive hepatocytes (Fig.3F, Suppl.Fig.7C–F). Likewise, CRISPRi of *Tead2* and *Tead4*, but not of *Tead1* or *Tead3*, in TAZ-driven hepatocarcinogenesis model significantly reduced hepatocyte proliferation 4 weeks after HTVI (Suppl.Fig.7G). TAZ deletion, or *Tead2* or *Tead4* CRISPRi did not affect liver fibrosis, inflammation and immune cell infiltration in tumors from DEN+CCl_4, CTNNB1-S45Y or TAZ-S89A HCC models (Suppl.Fig.2C–D, Suppl.Fig.7H–I). Together, these results suggest that the cholesterol biosynthesis-TAZ-TEAD pathway induces proliferation and possibly DNA damage, thereby contributing to hepatocyte transformation and HCC development.

ANLN, KIF23 and PD-L1 are tumor-promoting TAZ targets.

To examine the downstream target genes through which TAZ mediates HCC development, we performed *in vivo* CRISPR interference (CRISPRi) screening using dCas9 transgenic mice[38,39], focusing on known YAP/TAZ/TEAD target genes that were most upregulated in TAZ+CCl_4-induced tumors versus normal liver in RNA-seq (Suppl.Table.3). A library of TAZ-S89A-expressing plasmids, co-expressing gRNAs for 36 TAZ target genes (at five-fold coverage) and controls (Suppl.Table.1), was injected via HTVI into dCas9 mice, followed by 14 injections of CCl_4 and sequencing of livers 7 weeks after HTVI. We identified gRNAs targeting *Anln* and *Kif23* as the most depleted gRNAs in the screen and gRNAs targeting *Cdkn2a* as the most enriched gRNAs (4A, Suppl.Table.2). Of note, ANLN and KIF23 have been reported to play a role in the development of liver cancer [40–42] and high expression is associated with worse overall survival (Suppl.Fig.5A–B). Moreover, Anln and Kif23 were increased in mouse tdTom-labled TAZ-GFP-overexpressing primary hepatocytes (Suppl.Fig.8A). To validate ANLN and KIF23 as direct targets of TAZ, we next performed *in vivo* ChIP analysis, which showed significant enrichment of both *Anln* and *Kif23* sequences (Fig.4B) after Flag-IP in pT3-FLAG-TAZS89A-transduced HCC. To functionally test the role of ANLN and KIF23 in TAZ-driven HCC, we injected dCas9-transgenic mice with pT3-TAZ-S89A plasmid, co-expressing sgAnln and sgKif23, which had been validated in dCas9-transgenic cell lines (Suppl.Fig.8B). Both sgAnln and sgKif23 completely blocked TAZ-induced HCC (Fig.4C). Similar to the TAZ-S89-induced HCC, we found that *Anln* or *Kif23* knockdown almost completely prevented MET-CTNNB1-Y45-driven HCC development (4D). CRISPRi of *Anln* and *Kif23* also reduced Ki67-positive hepatocyte at early time points when macroscopic tumors had not yet developed (Fig.4E). We next tested their functions in HCC cell lines *in vitro*. We found a significant but modest reduction of cell numbers in cells silenced for either *Anln* or *Kif23* (Fig.4F, Suppl.Fig.8C). These findings show that ANLN and KIF23 are not absolutely required for cell survival or

proliferation, consistent with published studies that did not show inhibited liver regeneration in mice with *Anln* knockdown[41]. *ANLN* and *KIF23* expression did not differ significantly between different etiologies of HCC in the TCGA dataset and human TMA cases, and expression levels affected survival or showed strong trends in both viral and non-viral HCC (Suppl.Fig.8D–F,H). Furthermore, we found that TAZ induced the expression of PD-L1 in isolated hepatocytes (Suppl.Fig.9A), consistent with previous studies that have shown PD-L1 to be a YAP/TAZ target gene[43,44]. CRISPRi of PD-L1 in TAZ-driven HCC showed a significant, but moderate reduction of HCC development (Suppl.Fig.9B–C). Together, these findings suggest that epithelial TAZ induces hepatocarcinogenesis by multiple targets and mechanisms, which include Anln/Kif23-mediated proliferation and, to a lesser extent, upregulation of PD-L1, likely leading to immunosuppression.

Targeting the mevalonate-TAZ pathway for HCC monotherapy or combination therapy.

To investigate the mevalonate-TAZ pathway as potential therapeutic target for HCC, we tested the effects HMGCR inhibitor simvastatin *in vivo*, which strongly reduced TAZ expression in multiple HCC lines (Suppl.Fig.10A). In DEN+CCl_4-induced HCC, simvastatin significantly reduced TAZ expression in HCC after 1 week of treatment (Fig.5A) and simvastatin-treated mice showed decreased HCC after 8 weeks of treatment (Fig.5B). The moderate inhibition of TAZ expression and effects on HCC may not only be due to the incomplete blocking of HMGCR by statins, but also because mechanosensitive signals such as TAZ in tumors may be activated by a wide range of other upstream signaling pathways. We next tested combination therapy consisting of simvastatin plus the multi-kinase inhibitors sorafenib or lenvatinib, which are current first-line therapies for HCC. Interestingly, sorafenib treatment – and, also, to a lesser degree, lenvatinib treatment – led to a significant increase in TAZ expression in PLC/PRF/5 cells but not in Huh7 cells (Suppl.Fig.10B). Simvastatin not only reduced sorafenib- and lenvatinib-induced TAZ induction, but also significantly lowered HCC cell viability when combined with Sorafenib in Huh7, PLC/PRF/5 and Hep3B (Suppl.Fig.10B–C). We next confirmed these findings *in vivo* in the DEN+CCl_4-induced HCC model, where the combination of simvastatin and sorafenib exerted significantly stronger effects on the liver-body weight ratio and tumor number than either agent alone (Fig.5C). As the most effective current therapies for HCC consist of combinations that include immune checkpoint inhibitors[7], we next investigated the effects of combining mevalonate-TAZ pathway inhibition by a statin with an ICI. Consistent with recent clinical trials[45,46], anti-PD-1 monotherapy did not affect MET+CTNNB-1-induced HCC development (Fig.5D), possibly due to CTNNB1-induced immune exclusion[47–49]. However, combination therapy with simvastatin and anti-PD-1 led to a significant reduction of HCC development (Fig.5D, Suppl.Fig.10D). Together, these data suggest that statin-mediated TAZ inhibition may be considered as novel therapeutic option for HCC, particularly in combination with current first-line therapies such as sorafenib or PD-1/PD-L1 inhibitor-containing combinations.

Targeting the TEAD pathway for HCC therapy

Because inhibition of the TAZ pathway by statin monotherapy was only moderately effective *in vitro* and *in vivo*, we next test the effects of direct TEAD inhibition on HCC growth using recently developed pan-TEAD inhibitors VT104 or VT107 (Suppl.Fig.11A)[50].

TEAD inhibitors reduced proliferation (Fig.6A) and inhibited the TAZ-TEAD pathway, as evidenced by reduced expression of TAZ-TEAD targets *ANLN*, *KIF23*, *ANKRD1*, *CTGF* and *CD274*, in HCC lines (Fig.6B, Suppl.Fig.11B–C). VT104 strongly suppressed *in vivo* HCC development, driven by MET+CTNNB1-S45Y, while VT107 exerted only minor effects (Fig.6C), which may be due to its much shorter half-life[50]. Consistent with the roles for TAZ and TEADs we observed by genetic deletion, overexpression or CRISPRi, VT104 significantly reduced Ki67+ proliferating as well as γH2AX-positive hepatocytes (Fig.6D). Based on these findings and the strong effects of tumor cell-specific TEAD inhibition via CRISPRi, TEAD inhibitors may represent a promising approach for tumor-cell targeted therapy of HCC. Since TEAD3 and TEAD4 also impacted HCC in mice and patients in addition to TEAD2 (Fig.3B–C, Suppl.Fig.4B, Suppl.Fig.5–6), pan-TEAD inhibition may be a suitable approach to target this potent tumor cellintrinsic pathway for HCC therapy.

DISCUSSION

Despite recent progress in the medical therapy of HCC, 5-year survival rates remain low and there is an urgent need to develop more efficient therapeutic approach. The currently most successful therapeutic approaches for HCC are targeting the tumor microenvironment and there is a paucity of drugs that efficiently target tumor cells. In addition to the heterogeneous nature of HCC, which makes it difficult to broadly target tumor cell-intrinsic pathways, less than 20% of HCCs contain druggable mutations[8]. Thus, identifying and targeting shared pathways that are activated in HCC with different mutational profiles may provide novel therapeutic opportunities. Our current study reveals the mevalonate-cholesterol-TAZ-TEAD2-Anln/Kif23 pathway as novel tumor-specific target for HCC therapy. While inhibition of this pathway by statins showed only modest therapeutic effects, combination of statins with ICI significantly decreased tumor growth. Importantly, pan-TEAD inhibitor VT104 strongly inhibited tumor growth. Our findings on the role of TAZ in mice are consistent with a previous study in similar models[51]. Together with the strong effects of tumor cell-specific CRISPRi-mediated inhibition of TEAD2, ANLN or KIF23, our findings suggest that therapeutic inhibition of the cholesterol-TAZ-TEAD2-Anln/Kif23 pathway should be further evaluated in patients including combination with ICI therapy. Notably, TAZ was active in about 60% of human HCC cases (Suppl.Fig.1C), suggesting that such therapies may be broadly applicable in HCC with different mutational profiles.

The strong effect of TAZ and TEAD2 was further highlighted by their ability to trigger high-grade HCC, making at least TAZ more potent than the majority of oncogenic drivers, which often require the activation or inactivation of two distinct pathways or have long latency[52]. The difference between TAZ and YAP cannot be simply explained by differential expression, as both are strongly increased in HCC as demonstrated by us and others[14–17,53]. It is conceivable that the higher potency of TAZ compared to YAP might be caused by differences in complex formation with TEADs and TEAD transcriptional activity. Of note, the TAZ-TEAD complex can form hetero-tetramers, resulting in higher transcriptional activity compared to the YAP-TEAD complex, which cannot form heterotetramers[54]. CRISPRi-mediated inhibition of TEADs revealed a central role for TEAD2, that was consistently seen in all investigated models, but showed also potential roles for TEAD3 and TEAD4, consistent with our findings in TCGA and ICGC cohorts, which revealed

strongest effects for TEAD2 but additional and less consistent roles for TEAD3 and TEAD4. Since TCGA data do not show appreciable differences in expression between different TEADs in HCC, it appears that either more efficient complex formation with TAZ and/or the activation of distinct targets underly the strong tumor-promoting effects of specific TEADs in HCC. Mechanistically, TAZ and its downstream mediator TEAD2 triggered proliferation and proliferation-associated DNA damage, which amends our studies on the role of TAZ and its target, *Cybb* in NAFLD[13].

Our study suggests that targeting TAZ, its upstream regulators or downstream mediators might represent novel therapeutic approaches for HCC. Consistent with the reduced HCC incidence and mortality in statin-treated patients[55,56], HMGCR inhibitor simvastatin inhibited TAZ expression and tumor growth *in vivo*. However, effects were only moderate despite statins strongly reducing HCC cell proliferation observed by us and others[57] and TAZ expression *in vitro*. The moderate effects on tumor growth are likely due to the partial inhibition of HMGCR by statins and additional pathways besides mevalonate-cholesterol feeding into TAZ activation *in vivo*. Accordingly, we recently showed that hepatocyte TAZ, induced by liver stiffness, plays an important role in HCC development[51]. While we identified additional mediators of TAZ activation in the mevalonate-cholesterol pathway that could serve as targets besides HMGCR, such as farnesyl pyrophosphate synthase and FDFT1, the multiplicity of pathways contributing to TAZ activation in tumors suggest that targeting downstream of TAZ may be more efficient for tumor therapy. Consistent with our finding on TEAD CRISPRi, we observed a significant suppression of MET+CTNNB1-S45Y-driven HCC development by pan-TEAD inhibitor VT104. Although we found significant tumor-inhibitory effects across different HCC models only for TEAD2, there were trends towards tumor reduction for TEAD3 and TEAD4 inhibition in MET+CTNNB1-S45Y model and strong effects of TEAD4 in TAZ-driven HCC. Moreover, the TCGA and ICGC cohorts revealed the strongest effects of TEAD2, but also moderate and less consistent effects of TEAD3 and TEAD4. Thus, pan-TEAD inhibitors like VT104 might be more suitable for HCC therapy than for example TEAD2-specific inhibition. Furthermore, our tumor cell-specific CRISPRi approaches demonstrated that the TAZ-TEAD pathway is a tumor cell-intrinsic tumor-promoting pathway and that targeting this pathway might therefore have synergistic effects if combined with highly efficient already approved TIME-targeting therapies.

Our CRISPRi screen and subsequent CRISPRi-mediated inhibition showed a potent role of TAZ downstream mediators in the tumor cell compartment. Inhibition of TAZ target genes *Anln* and *Kif23*, which were previously reported to promote HCC[40–42], nearly completely blocked HCC formation and proliferation, both in the TAZ- and MET-CTNNB1-S45Y-driven HCC models, and strongly improved survival in the MET-CTNNB1-S45Y-driven HCC model. These findings and the lack of requirement for ANLN and KIF23 for normal hepatocyte proliferation, as seen in models of liver regeneration[40,41], render ANLN and KIF23 attractive therapeutic targets in HCC. Because as yet there are no known specific inhibitors for these molecules, GalNAc-coupled siRNA, an FDA-approved hepatocyte-specific delivery approach[58,59], or nanoparticle-mediated delivery of siRNA to the liver could be used for primary or secondary prevention of HCC with high expression of TAZ[40,41]. Since the effects of *Kif23* and *Anln* CRISPRi were much more potent than

pan-TEAD inhibitors, it is important to determine if KIF23 and ANLN are regulated by pathways besides TAZ or whether pan-TEAD inhibitors did not completely block TEAD activity, suggesting that drug chemistry, dosing or delivery to tumor cells may need to be further improved.

Our study has several limitations. While we saw a prominent role for TEAD2 in CRISPRi studies, our CRISPRi screen did not clearly reveal *Tead2* as opposed to TAZ targets *Anln* and *Kif23*. This is likely due to insufficient power of our screening method to detect mediators with weaker effects or a higher level of redundancy in the case of TEADs. As such, our top hits in this screen, *Anln* and *Kif23*, nearly completely prevented TAZ-induced HCC formation. A second limitation is the relatively early start of statin plus ICI or pan-TEAD inhibitors treatment, and the lack of survival studies in mice. Future studies need to fill these gaps and determine whether the TAZ-TEAD2-ANLN/KIF23 pathway can be targeted for tumor prevention, tumor therapy or both. Also, future studies should investigate the combination of pan-TEAD inhibitors with ICI to prove our underlying concept that combining tumor cell-targeted therapies with TIME-targeted therapies is synergistic and that such combination may provide further benefits to patients with HCC.

Supplementary Material

Refer to Web version on PubMed Central for supplementary material.

ACKNOWLEDGEMENTS

We would like to thank Dr. Silvia Affo (Hospital Clínic Barcelona) for help with HTVI, Deqi Yin (Columbia University) for help with mouse colonies, Drs. Xin Chen (University of Hawaii), Paul Monga (University of Pittsburgh) for providing plasmids and Tracy T. Tang (Vivace Therapeutics) for providing pan-TEAD inhibitors, VT104 and VT107.

Grant support:

This work was supported by National Institutes of Health, National Cancer Institute grants R01CA190844 and R01CA228483 (to Robert F. Schwabe), National Institute of Diabetes and Digestive and Kidney Diseases grant R01DK116620 (to Robert F. Schwabe and Ira Tabas), and the Columbia University Digestive and Liver Disease Research Center award 1P30DK132710 from the National Institute of Diabetes and Digestive and Kidney Diseases; the Arnold and Mabel Beckman Foundation, National Institute of Diabetes and Digestive and Kidney Diseases grant R03DK123543 and National Cancer Institute grant 1R37CA259201 (to Kirk J. Wangensteen); and National Institutes of Health, National Cancer Institute grants R01CA233794 and R01CA255621, and Cancer Prevention and Research Institute of Texas grant RR180016 (to Yujin Hoshida). Yoshinobu Saito was supported by fellowships from the Uehara Memorial Foundation and the Naomi Berrie Diabetes Center Russell Berrie Foundation. Aveline Filliol was funded by a Fondation pour la Recherche Médicale fellowship (SPE20170336778), an American Liver Foundation Postdoctoral Research Award, an International Liver Cancer Association's Fellowship, and the Mandl Connective Tissue Research Fellowship. Xiaobo Wang was supported by an American Liver Foundation Liver Scholar Award.

Disclosure:

The authors disclose no conflicts.

Abbreviations:

AAV	Adeno-associated virus
AFP	alpha fetoprotein

ANLN	anillin
BW	body weight
CDAA	choline-deficient L-amino acid
ChIP	chromatin immunp- precipitation
CRISPRi	Clustered Regularly Interspaced Short Palindromic Repeats interference
dCas9	nuclease dead Cas9
DEN	diethylnitrosamine
DMSO	dimethyl sulfoxide
dnTEAD2	dominant negative TEA domain transcription factor 2
FACS	fluorescence activated cell sorting
FDFT1	farnesyl-diphosphate farnesyltransferase 1
FPP	farnesyl pyrophosphate ammonium salt
FPPS	farnesyl pyrophosphate synthase
GGPP	geranylgeranyl pyrophosphate ammonium salt
gRNA	guide RNA
HCC	hepatocellular carcinoma
HMGCR	3-hydroxy-3-methylglutaryl-CoA reductase
HTVI	hydrodynamic tail vein injection
ICI	immune checkpoint inhibitors
LW	liver weight
KIF23	kinesin family member 23
NAFLD	non-alcoholic fatty liver disease
NASH	non-alcoholic steatohepatitis
PBS	phosphate buffered saline
PD-L1	programmed cell death ligand 1
SREBP2	sterol regulatory element-binding protein 2
TBG	thyroid hormone-binding globulin
TEAD	TEA domain transcription factor

TMA	tissue micro array
TIME	tumor immune microenvironment
VEGF	vascular endothelial growth factor

REFERENCES

1. Villanueva A. Hepatocellular Carcinoma. N Engl J Med 2019;380:1450–1462. [PubMed: 30970190]
2. Ryerson AB, Eheman CR, Altekruse SF, et al. Annual Report to the Nation on the Status of Cancer, 1975–2012, featuring the increasing incidence of liver cancer. Cancer 2016;122:1312–37. [PubMed: 26959385]
3. Jemal A, Ward EM, Johnson CJ, et al. Annual Report to the Nation on the Status of Cancer, 1975–2014, Featuring Survival. J Natl Cancer Inst 2017;109.
4. Llovet JM, Ricci S, Mazzaferro V, et al. Sorafenib in advanced hepatocellular carcinoma. N Engl J Med 2008;359:378–90. [PubMed: 18650514]
5. El-Khoueiry AB, Sangro B, Yau T, et al. Nivolumab in patients with advanced hepatocellular carcinoma (CheckMate 040): an open-label, non-comparative, phase 1/2 dose escalation and expansion trial. Lancet 2017;389:2492–2502. [PubMed: 28434648]
6. Finn RS, Qin S, Ikeda M, et al. Atezolizumab plus Bevacizumab in Unresectable Hepatocellular Carcinoma. N Engl J Med 2020;382:1894–1905. [PubMed: 32402160]
7. Llovet JM, Kelley RK, Villanueva A, et al. Hepatocellular carcinoma. Nat Rev Dis Primers 2021;7:6. [PubMed: 33479224]
8. Hyman DM, Taylor BS, Baselga J. Implementing Genome-Driven Oncology. Cell 2017;168:584–599. [PubMed: 28187282]
9. Moroishi T, Hansen CG, Guan KL. The emerging roles of YAP and TAZ in cancer. Nat Rev Cancer 2015;15:73–79. [PubMed: 25592648]
10. Zhang S, Zhou D. Role of the transcriptional coactivators YAP/TAZ in liver cancer. Curr Opin Cell Biol 2019;61:64–71. [PubMed: 31387016]
11. Wang X, Zheng Z, Caviglia JM, et al. Hepatocyte TAZ/WWTR1 Promotes Inflammation and Fibrosis in Nonalcoholic Steatohepatitis. Cell Metab 2016;24:848–862. [PubMed: 28068223]
12. Wang X, Cai B, Yang X, et al. . Cholesterol Stabilizes TAZ in Hepatocytes to Promote Experimental Non-alcoholic Steatohepatitis. Cell Metab 2020;31:969–986 e7. [PubMed: 32259482]
13. Wang X, Zeldin S, Shi H, et al. TAZ-induced Cybb contributes to liver tumor formation in non-alcoholic steatohepatitis. J Hepatol 2022;76:910–920. [PubMed: 34902531]
14. Guo Y, Pan Q, Zhang J, et al. Functional and clinical evidence that TAZ is a candidate oncogene in hepatocellular carcinoma. J Cell Biochem 2015;116:2465–75. [PubMed: 25650113]
15. Van Haele M, Moya IM, Karaman R, et al. YAP and TAZ Heterogeneity in Primary Liver Cancer: An Analysis of Its Prognostic and Diagnostic Role. Int J Mol Sci 2019;20. [PubMed: 31861461]
16. Liu-Chittenden Y, Huang B, Shim JS, et al. Genetic and pharmacological disruption of the TEAD-YAP complex suppresses the oncogenic activity of YAP. Genes Dev 2012;26:1300–5. [PubMed: 22677547]
17. Fitamant J, Kottakis F, Benhamouche S, et al. YAP Inhibition Restores Hepatocyte Differentiation in Advanced HCC, Leading to Tumor Regression. Cell Rep 2015;10:1692–1707. [PubMed: 25772357]
18. Moya IM, Castaldo SA, Van den Mooter L, et al. Peritumoral activation of the Hippo pathway effectors YAP and TAZ suppresses liver cancer in mice. Science 2019;366:1029–1034. [PubMed: 31754005]
19. Wangensteen KJ, Wilber A, Keng VW, et al. A facile method for somatic, lifelong manipulation of multiple genes in the mouse liver. Hepatology 2008;47:1714–24. [PubMed: 18435462]
20. Piccolo S, Dupont S, Cordenonsi M. The biology of YAP/TAZ: hippo signaling and beyond. Physiol Rev 2014;94:1287–312. [PubMed: 25287865]

21. Moya IM, Halder G. Hippo-YAP/TAZ signalling in organ regeneration and regenerative medicine. Nat Rev Mol Cell Biol 2019;20:211–226. [PubMed: 30546055]
22. Wang H, Zhang S, Zhang Y, et al. TAZ is indispensable for c-MYC-induced hepatocarcinogenesis. J Hepatol 2022;76:123–134. [PubMed: 34464659]
23. Totaro A, Panciera T, Piccolo S. YAP/TAZ upstream signals and downstream responses. Nat Cell Biol 2018;20:888–899. [PubMed: 30050119]
24. Sorrentino G, Ruggeri N, Specchia V, et al. Metabolic control of YAP and TAZ by the mevalonate pathway. Nat Cell Biol 2014;16:357–66. [PubMed: 24658687]
25. Horton JD, Goldstein JL, Brown MS. SREBPs: activators of the complete program of cholesterol and fatty acid synthesis in the liver. J Clin Invest 2002;109:1125–31. [PubMed: 11994399]
26. Madison BB. Srebp2: A master regulator of sterol and fatty acid synthesis. J Lipid Res 2016;57:333–5. [PubMed: 26798145]
27. Moon SH, Huang CH, Houlihan SL, et al. p53 Represses the Mevalonate Pathway to Mediate Tumor Suppression. Cell 2019;176:564–580.e19. [PubMed: 30580964]
28. Kawamura S, Matsushita Y, Kurosaki S, et al. Inhibiting SCAP/SREBP exacerbates liver injury and carcinogenesis in murine nonalcoholic steatohepatitis. J Clin Invest 2022;132.
29. Dey A, Varelas X, Guan KL. Targeting the Hippo pathway in cancer, fibrosis, wound healing and regenerative medicine. Nat Rev Drug Discov 2020;19:480–494. [PubMed: 32555376]
30. Alarcon C, Zaromytidou AI, Xi Q, et al. Nuclear CDKs drive Smad transcriptional activation and turnover in BMP and TGF-beta pathways. Cell 2009;139:757–69. [PubMed: 19914168]
31. Varelas X, Sakuma R, Samavarchi-Tehrani P, et al. TAZ controls Smad nucleocytoplasmic shuttling and regulates human embryonic stem-cell self-renewal. Nat Cell Biol 2008;10:837–48. [PubMed: 18568018]
32. Varelas X, Samavarchi-Tehrani P, Narimatsu M, et al. . The Crumbs complex couples cell density sensing to Hippo-dependent control of the TGF-beta-SMAD pathway. Dev Cell 2010;19:831–44. [PubMed: 21145499]
33. Murakami M, Nakagawa M, Olson EN, et al. A WW domain protein TAZ is a critical coactivator for TBX5, a transcription factor implicated in Holt-Oram syndrome. Proc Natl Acad Sci U S A 2005;102:18034–9. [PubMed: 16332960]
34. Zhang H, Liu CY, Zha ZY, et al. TEAD transcription factors mediate the function of TAZ in cell growth and epithelial-mesenchymal transition. J Biol Chem 2009;284:13355–62. [PubMed: 19324877]
35. Wangensteen KJ, Wang YJ, Dou Z, et al. Combinatorial genetics in liver repopulation and carcinogenesis with a in vivo CRISPR activation platform. Hepatology 2018;68:663–676. [PubMed: 29091290]
36. Zhang J, Liu P, Tao J, et al. TEA Domain Transcription Factor 4 Is the Major Mediator of Yes-Associated Protein Oncogenic Activity in Mouse and Human Hepatoblastoma. Am J Pathol 2019;189:1077–1090. [PubMed: 30794805]
37. Mooring M, Fowl BH, Lum SZC, et al. Hepatocyte Stress Increases Expression of Yes-Associated Protein and Transcriptional Coactivator With PDZ-Binding Motif in Hepatocytes to Promote Parenchymal Inflammation and Fibrosis. Hepatology 2020;71:1813–1830. [PubMed: 31505040]
38. Larson MH, Gilbert LA, Wang X, et al. CRISPR interference (CRISPRi) for sequence-specific control of gene expression. Nat Protoc 2013;8:2180–96. [PubMed: 24136345]
39. Kieckhaefer JE, Maina F, Wells RG, et al. Liver Cancer Gene Discovery Using Gene Targeting, Sleeping Beauty, and CRISPR/Cas9. Semin Liver Dis 2019;39:261–274. [PubMed: 30912094]
40. Zhang S, Nguyen LH, Zhou K, et al. Knockdown of Anillin Actin Binding Protein Blocks Cytokinesis in Hepatocytes and Reduces Liver Tumor Development in Mice Without Affecting Regeneration. Gastroenterology 2018;154:1421–1434. [PubMed: 29274368]
41. Lin YH, Zhang S, Zhu M, et al. Mice With Increased Numbers of Polyploid Hepatocytes Maintain Regenerative Capacity But Develop Fewer Hepatocellular Carcinomas Following Chronic Liver Injury. Gastroenterology 2020;158:1698–1712 e14. [PubMed: 31972235]
42. Sun X, Jin Z, Song X, et al. Evaluation of KIF23 variant 1 expression and relevance as a novel prognostic factor in patients with hepatocellular carcinoma. BMC Cancer 2015;15:961. [PubMed: 26674738]

43. Janse van Rensburg HJ, Azad T, Ling M, et al. The Hippo Pathway Component TAZ Promotes Immune Evasion in Human Cancer through PD-L1. Cancer Res 2018;78:1457–1470. [PubMed: 29339539]
44. Nguyen CDK, Yi C. YAP/TAZ Signaling and Resistance to Cancer Therapy. Trends Cancer 2019;5:283–296. [PubMed: 31174841]
45. Finn RS, Ryoo BY, Merle P, et al. Pembrolizumab As Second-Line Therapy in Patients With Advanced Hepatocellular Carcinoma in KEYNOTE-240: A Randomized, Double-Blind, Phase III Trial. J Clin Oncol 2020;38:193–202. [PubMed: 31790344]
46. Yau T, Park JW, Finn RS, et al. Nivolumab versus sorafenib in advanced hepatocellular carcinoma (CheckMate 459): a randomised, multicentre, open-label, phase 3 trial. Lancet Oncol 2022;23:77–90. [PubMed: 34914889]
47. Harding JJ, Nandakumar S, Armenia J, et al. Prospective Genotyping of Hepatocellular Carcinoma: Clinical Implications of Next-Generation Sequencing for Matching Patients to Targeted and Immune Therapies. Clin Cancer Res 2019;25:2116–2126. [PubMed: 30373752]
48. Luke JJ, Bao R, Sweis RF, et al. WNT/beta-catenin Pathway Activation Correlates with Immune Exclusion across Human Cancers. Clin Cancer Res 2019;25:3074–3083. [PubMed: 30635339]
49. Ruiz de Galarreta M, Bresnahan E, Molina-Sanchez P, et al. beta-Catenin Activation Promotes Immune Escape and Resistance to Anti-PD-1 Therapy in Hepatocellular Carcinoma. Cancer Discov 2019;9:1124–1141. [PubMed: 31186238]
50. Tang TT, Konradi AW, Feng Y, et al. Small Molecule Inhibitors of TEAD Auto-palmitoylation Selectively Inhibit Proliferation and Tumor Growth of NF2-deficient Mesothelioma. Mol Cancer Ther 2021;20:986–998. [PubMed: 33850002]
51. Filliol A, Saito Y, Nair A, et al. Opposing roles of hepatic stellate cell subpopulations in hepatocarcinogenesis. Nature 2022;610:356–365. [PubMed: 36198802]
52. Caviglia JM, Schwabe RF. Mouse models of liver cancer. Methods Mol Biol 2015;1267:165–83. [PubMed: 25636469]
53. Han SX, Bai E, Jin GH, et al. Expression and clinical significance of YAP, TAZ, and AREG in hepatocellular carcinoma. J Immunol Res 2014;2014:261365.
54. Kaan HYK, Chan SW, Tan SKJ, et al. Crystal structure of TAZ-TEAD complex reveals a distinct interaction mode from that of YAP-TEAD complex. Sci Rep 2017;7:2035. [PubMed: 28515457]
55. Singh S, Singh PP, Singh AG, et al. Statins are associated with a reduced risk of hepatocellular cancer: a systematic review and meta-analysis. Gastroenterology 2013;144:323–32. [PubMed: 23063971]
56. Simon TG, Duberg AS, Aleman S, et al. Lipophilic Statins and Risk for Hepatocellular Carcinoma and Death in Patients With Chronic Viral Hepatitis: Results From a Nationwide Swedish Population. Ann Intern Med 2019;171:318–327. [PubMed: 31426090]
57. Higashi T, Hayashi H, Kitano Y, et al. Statin attenuates cell proliferative ability via TAZ (WWTR1) in hepatocellular carcinoma. Med Oncol 2016;33:123. [PubMed: 27734263]
58. Ledford H. Gene-silencing technology gets first drug approval after 20-year wait. Nature 2018;560:291–292. [PubMed: 30108348]
59. Adams D, Gonzalez-Duarte A, O'Riordan WD, et al. Patisiran, an RNAi Therapeutic, for Hereditary Transthyretin Amyloidosis. N Engl J Med 2018;379:11–21. [PubMed: 29972753]

WHAT YOU NEED TO KNOW

Background and context:

TEA domain transcription factors (TEADs), anillin (ANLN), transcriptional coactivator with PDZ-binding motif (TAZ), and Yes-associated protein (YAP) are activated in many cancers, but their role and regulation in hepatocellular carcinoma development are insufficiently understood.

New findings:

TAZ and YAP expression are regulated by the cholesterol synthesis pathway in HCC. TAZ, not YAP, potently promotes HCC growth via a TAZ-TEAD2-ANLN/KIF23 pathway. Therapeutic targeting of this pathway via pan-TEAD inhibition as well as through statins either alone or in combination with sorafenib or immune checkpoint inhibitor significantly reduced tumor growth.

Limitations:

The effect of combining pan-TEAD inhibitors with immune checkpoint inhibitors was not tested. Some studies in mice did not include survival analysis.

Clinical Research Relevance:

Targeting the TAZ-TEAD2 pathway combined with current first-line therapies may be synergistic for HCC therapy. TEAD inhibition may open up a novel HCC therapy.

Basic Research Relevance:

The TAZ-TEAD2 pathway may represent a cancer cell-intrinsic therapeutic target that could potentially be synergistic in combination with tumor microenvironment- and immune-targeted therapies.

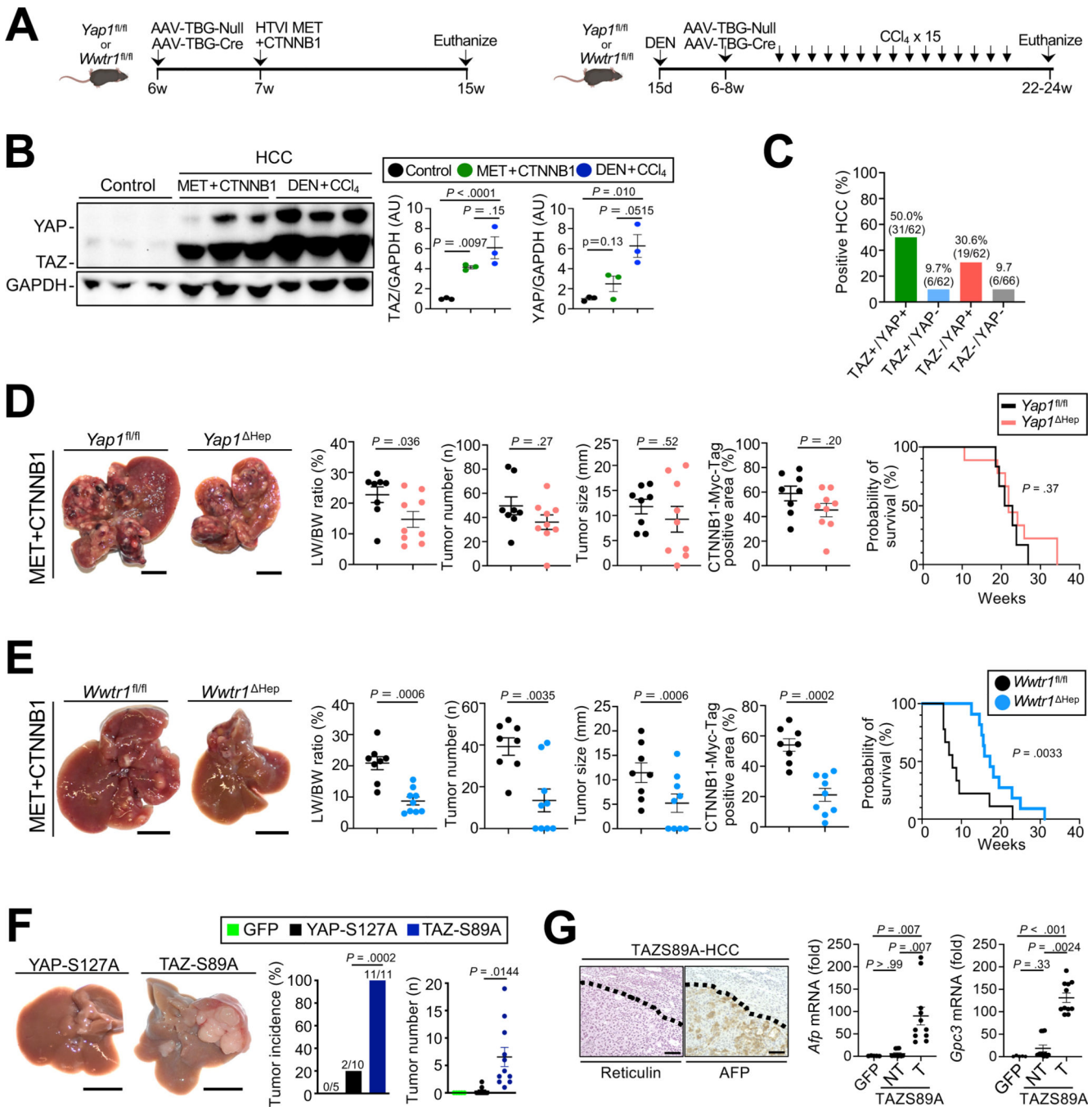

Figure 1. TAZ, not YAP, inhibition reduces HCC development and mortality.

A. Schematic of experimental procedures for MET+CTNNB1S45Y- and DEN+CCl_4–induced HCC models. **B.** Western blotting and quantification of TAZ and YAP in normal liver and HCC induced by MET+CTNNB1S45Y or DEN+CCl_4. **C.** Determination of TAZ and YAP in human HCC on a TMA. **D.** Effects of hepatocyte-specific deletion of YAP on MET+CTNNB1S45Y-induced HCC (n=8 *Yap1*$^{fl/fl}$ and n=9 *Yap1*$^{\Delta Hep}$ mice) as shown by representative images, LW/BW ratio, tumor number and tumor size, as well as survival (n=6 *Yap1*$^{fl/fl}$ and n=9 *Yap1*$^{\Delta Hep}$ mice). **E.** Evalution of hepatocyte-specific deletion of

TAZ on MET+CTNNB1S45Y-induced HCC (n=8 *Wwtr1*$^{fl/fl}$ and n=9 *Wwtr1*$^{\Delta Hep}$ mice) as described above and determination of survival (n=9 *Wwtr1*$^{fl/fl}$ and n=11 *Wwtr1*$^{\Delta Hep}$ mice). **F-G.** Representative liver images, tumor incidence and number of mice 4 months after HTVI of GFP (n=5), YAP S127A (n=10) or TAZ-S89A (n=11) (F) as well as reticulin and AFP staining and expression of *Afp* and *Gpc3* mRNA (G). NT, non-tumor; T, tumor. Scale bar (**D-F**): 1 cm, (**G**): 100 μm.

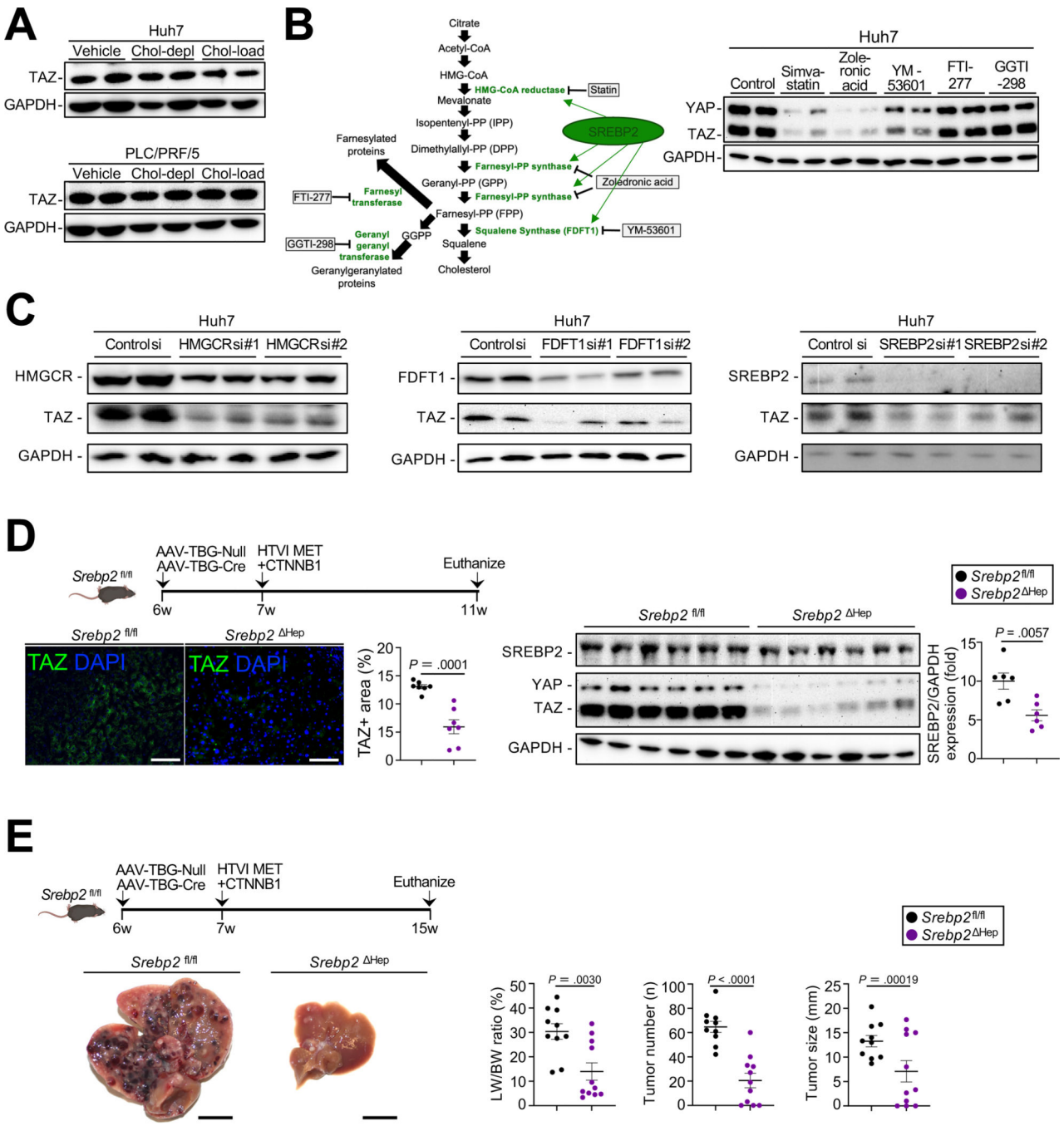

Figure 2. The mevalonate-squalene-cholesterol biosynthesis pathway regulates TAZ expression in HCC.

A. Following cholesterol depletion, Huh7 and PLC/PRF/5 cells were incubated with cholesterol-enriched liposomes, and TAZ expression was assessed by WB. **B.** Schematic of the mevalonate pathway and pharmacologic inhibitors. TAZ and YAP expression assessed by WB in Huh7 treated with inhibitors of the mevalonate pathway. **C.** Effect of *HMGCR*, *FDFT1* and *SREBP2* silencing on TAZ expression in Huh7 cells. **D,E.** SREBP2 deletion in the MET+CTNNB1S45Y model. TAZ expression assessed by WB and immunofluorescent

staining (n=7 *Srebp2*$^{fl/fl}$ and n=7 *Srebp2*$^{\Delta Hep}$ mice) (D). HCC development was assessed by LW/BW ratio, tumor number and tumor size (E, n=10 *Srebp2*$^{fl/fl}$ and n=11 *Srebp2*$^{\Delta Hep}$ mice). Scale bar (**D**): 100 μm, (**E**): 1 cm.

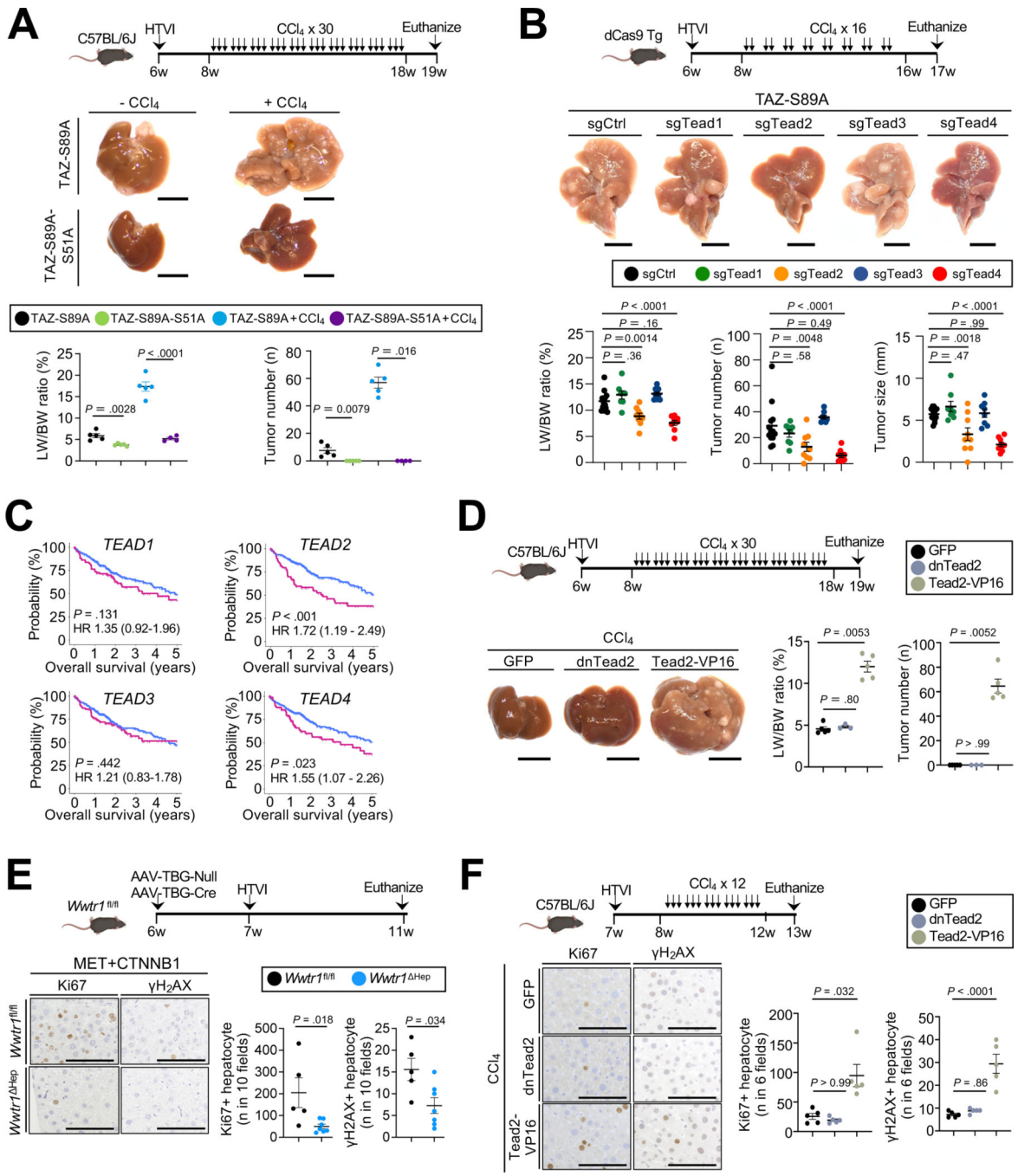

Figure 3. TAZ-TEAD2 interaction is crucial for HCC development by inducing proliferation.

A. Representative images, LW/BW ratio and tumor number (n=4–5 per group) from C57Bl/6 mice after HTVI of TAZ-S89A and TAZ-S89A-S51A (lacking interaction with TEADs) ± CCl_4 (3 injections/week for 10 weeks). **B.** Representative images, LW/BW ratio, tumor number and size from dCas9 transgenic mice after HTVI of TAZ-S89A-sgCtrl/Tead1/Tead2/Tead3/Tead4 plasmids (n=13 sgCtrl, n=8 sgTead1, n=9 sgTead2, n=8 sgTead3 and n=9 sgTead4 mice) followed by CCl_4 injections (2x/week for 8 weeks). **C.** Survival of HCC patients from the TCGA-LIHC cohort, stratified by expression of TEAD1, TEAD2, TEAD3

and TEAD4. **D.** Representative images, LW/BW ratio, tumor number and tumor size from C57BL/6J mice after HTVI of GFP (n=5 mice), dnTead2 (n=3 mice) and Tead2-VP16 (n=5 mice) plasmids, followed by CCl4 injection as depicted. **E-F.** Representative images and quantification of Ki67-and γH2AX-positive hepatocytes in *Wwtr1*$^{fl/fl}$ (n=5) or *Wwtr1*$^{\Delta Hep}$ (n=6) mice 4 weeks after HTVI of MET+CTNNB1S45Y plasmids (E) or C57BL/6J mice after HTVI of GFP, dnTead2 or Tead2-VP16 plasmids (n=5/group), followed by CCl_4 as depicted (F). Scale bar (**A,B,D**): 1 cm, (**E,F**): 100 μm

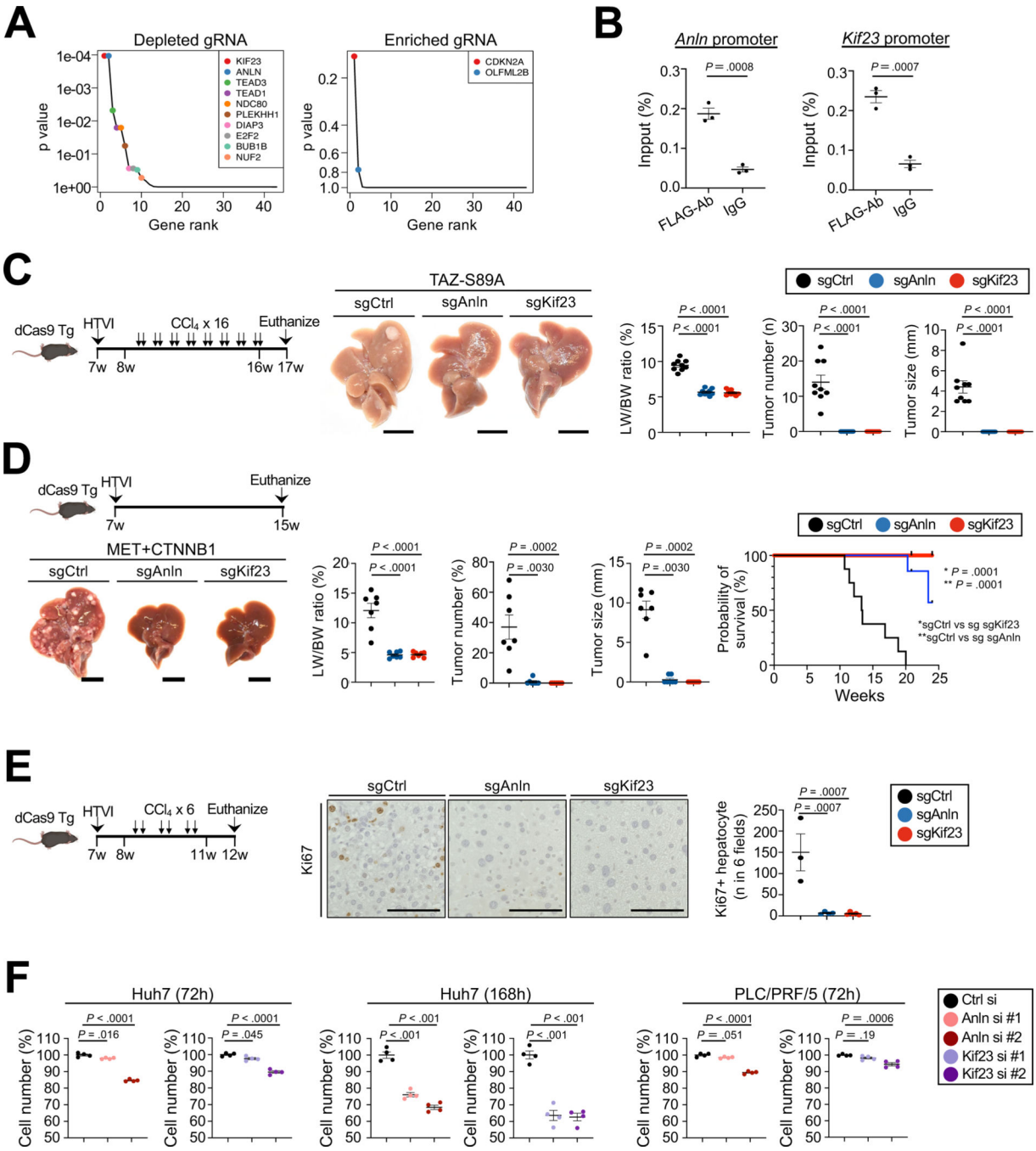

Figure 4. TAZ target genes *Anln* and *Kif23* drive HCC growth.

A. Results of CRISPRi screening of 36 TAZ target genes or downstream mediators. p value is adjusted by false discovery rate. **B.** ChIP in extracts from TAZ-S89A-Flag-transduced HCCs, using FLAG antibody or IgG followed by qPCR for the *Anln* and *Kif23* promoter. Data were normalized by values obtained from input DNA (n=3/group) **C.** Representative images, LW/BW ratio, tumor number and size from dCas9 transgenic mice after HTVI of TAZS89A-sgCtrl/Anln/Kif23 plasmids (n=9 sgCtrl, n=9 sgAnln, n=8 sgKif23 mice) followed by CCl_4 injection as depicted. **D.** Evaluation of HCC as described above and

survival of dCas9 transgenic mice 8 weeks after HTVI with MET-sgCont/Anln/Kif23 and CTNNB1-S45Y plasmids (n=7 sgCtrl, n=7 sgAnln, n=7 sgKif23 mice for tumor growth; n=8 sgCtrl, n=7 sgAnln, n=7 sgKif23 mice for survival studies). **E.** Quantification of Ki67-positive hepatocytes in dCas9 transgenic mice after HTVI of TAZS89A-sgCont/Anln/Kif23 plasmids (n=3 sgCtrl, n=4 sgAnln, n=4 sgKif23) as depicted. **F.** siRNA-mediated knockdown of *ANLN* or *KIF23* in Huh7 and PLCR/PRF5, followed by WST assay to assess cell numbers. *sgCtrl vs sg sgAnln. **sgCtrl vs sg sgKif23. Scale bar (**C, D**): 1 cm, (**E**): 100μm.

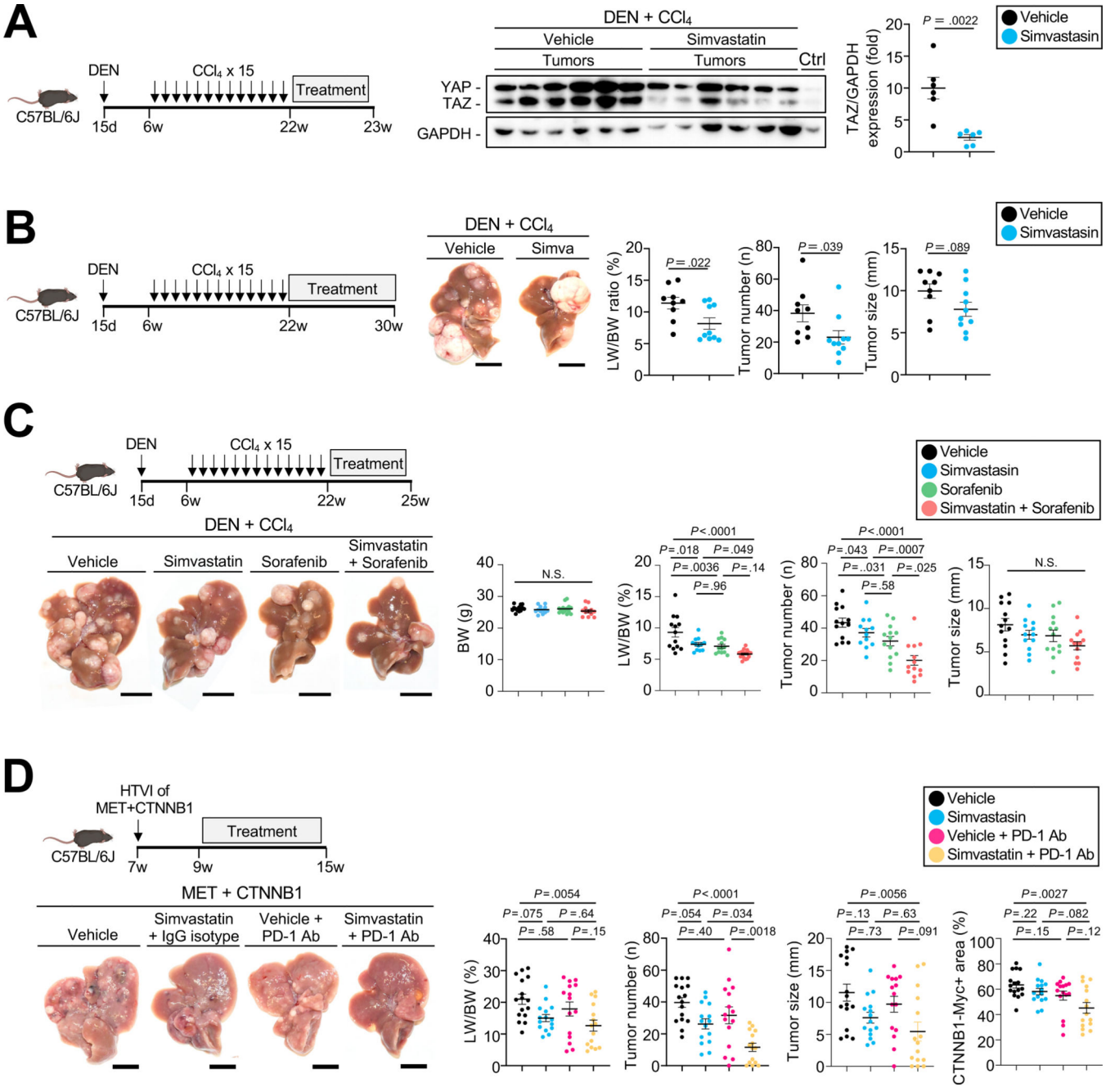

Figure 5. Targeting the mevalonate-TAZ pathway for HCC therapy with or without multi-kinase and immune checkpoint inhibitor.

A. YAP and TAZ expression assessed by WB in mice treated with simvastatin or vehicle (n=6 each) for 1 week. **B.** Representative images, LW/BW ratio, tumor number and tumor size from DEN+CCl_4-injected mice treated with vehicle (n=9) or simvastatin (n=10) for 8 weeks. **C.** Determination of BW, LW/BW ratio, tumor number and size in DEN+CCl_4-injected mice treated with vehicle (n=13), simvastatin (n=12), sorafenib (n=13), or sorafenib plus simvastatin (n=13) for three weeks. **D.** Representative images, LW/BW ratio, tumor number and size and CTNNB1-Myc-Tag-positive area from C57BL/6J mice after HTVI

with MET+CTNNB1-S45Y followed by treatment with vehicle (n=16), simvastatin+IgG isotype control (n=15), vehicle+anti-PD-1 (n=15) or simvastatin+anti-PD1 (n=15) 2 weeks after HTVI, as described in the materials and methods. Scale bar (**B,C,D**): 1 cm.

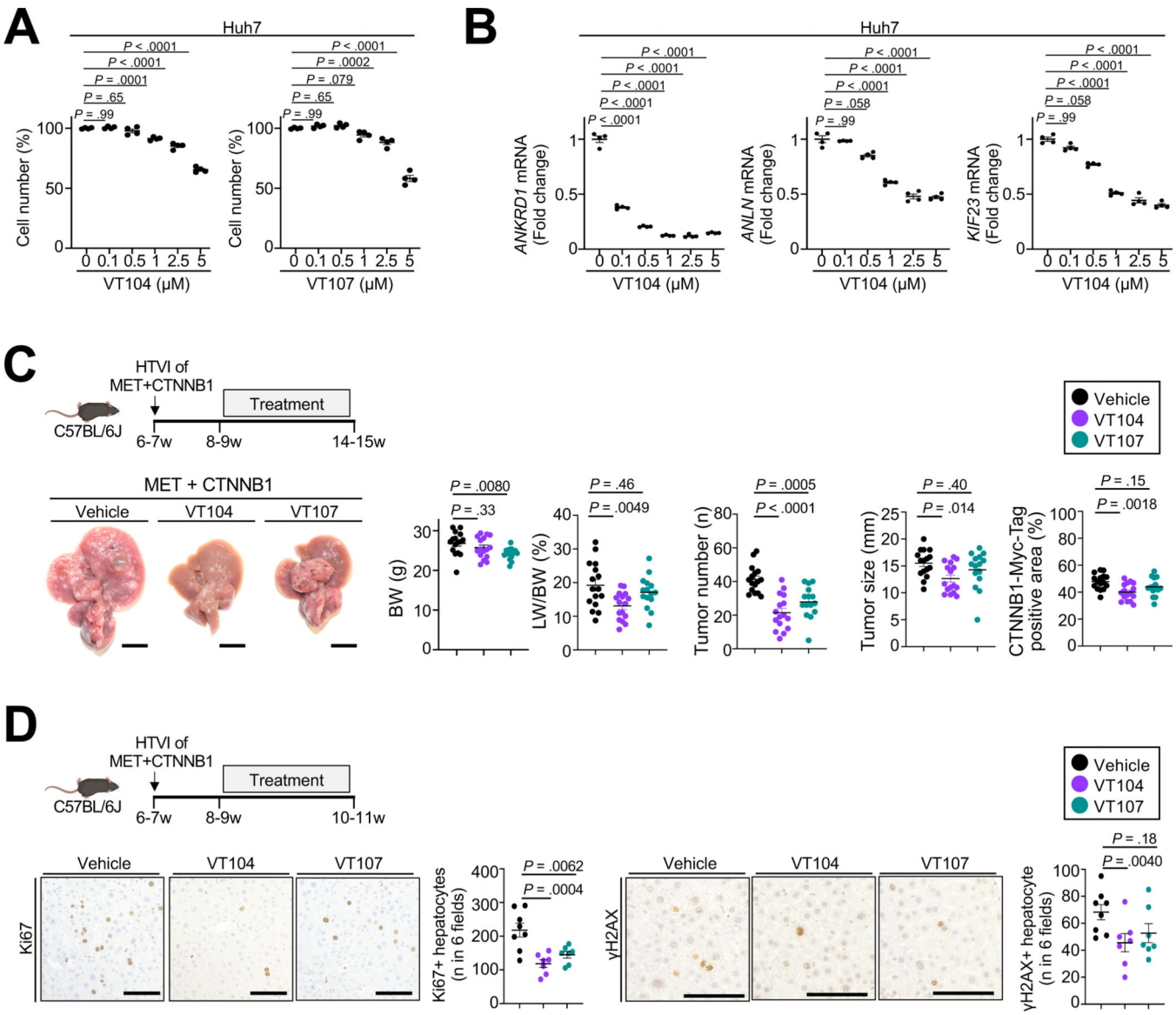

Figure 6. TEAD inhibitors suppressed HCC development.

A,B. Huh7 cells were treated with pan-TEAD inhibitor VT104 for 72h (A) followed by WST assay to assess cell number or for 24h for qPCR of *ANKRD1*, *ANLN* and *KIF23*.

C,D. Representative images, LW/BW ratio, tumor number and size and CTNNB1-Myc-Tag-positive area from C57BL/6J mice after HTVI of MET+CTNNB1-S45Y, followed by treatment with vehicle (n=16), pan-TEAD inhibitors VT104 (n=16, 10 mg/kg/day) or VT107 (n=15, 30 mg/kg/day) for 6 weeks (C) as well as representative images and quantification of Ki67 and γH2AX staining after treatment with vehicle (n=8) or pan-TEAD inhibitors VT104 (n=7) or VT107 (n=7) for 2 weeks (D). Scale bar (**C**): 1 cm, (**D**): 100μm.